Thermochimica Acta 472 (2008) 55–63

Contents lists available at ScienceDirect

Thermochimica Acta

journal homepage: www.elsevier.com/locate/tca

Effect of the heating rate on the devolatilization of biomass residues

E. Biagini[a,*], A. Fantei[b], L. Tognotti[b]

[a] Consorzio Pisa Ricerche, Divisione Energia e Ambiente – Lungarno Mediceo 40, 56127 Pisa, Italy
[b] Dipartimento di Ingegneria Chimica – Università di Pisa – via Diotisalvi 2, 56122 Pisa, Italy

ARTICLE INFO

Article history:
Received 7 December 2007
Received in revised form 14 March 2008
Accepted 24 March 2008
Available online 29 March 2008

Keywords:
Pyrolysis
Lignin–cellulose materials
Solid fuels
Thermal degradation
Kinetic analysis
Fundamental model

ABSTRACT

The devolatilization is the basic step of thermochemical processes and requires a fundamental characterization. Three biomass residues (rice husks, olive cake, cacao shells) are studied here in a thermogravimetric (TG) balance. The effect of the heating rate (HR) is evaluated in the range 5–100 K/min providing significant parameters for the fingerprinting of the fuels. Kinetics are obtained by applying traditional isoconversional methods. The activation energy as function of the conversion reveals the multi-step nature of the biomass devolatilization. Although average values allow the reactivity of different fuels to be compared, a first order reaction model can hardly predict the biomass devolatilization. A VEB (Variable activation Energy model for Biomass devolatilization) model is developed, basing on the results of the kinetic analysis. A good agreement is obtained for the biomass residues in all HR runs in the entire range of temperatures. Similarities in the optimized E_{VEB} curves for the three fuels of this work suggest to pursue a generalization in the approach, enlarging the number and variety of fuels studied.

1. Introduction

Agricultural and food residues represent a renewable energy source, may be abundant in specific local areas and cause disposal problems. Thermochemical processes constitute interesting options for biomass utilization [1–5]: co-combustion is a short time opportunity for benefitting the biomass advantages (CO_2 neutral fuels, low emissions of sulphur and heavy metals); gasification is a clean and efficient alternative for converting biomasses into upgraded fuels (syngas for direct energy generation or hydrogen production in a mid-term scenario); pyrolysis is a versatile process for recovering chemicals and fuels.

Devolatilization is the first step of all these thermochemical processes. It consists in the release of volatile matter (condensable and light gases) during the continuous heating of the solid fuel. The thermal scission of chemical bonds in the natural polymers (cellulose and lignin) causes the formation of cracked compounds (the lighter products passing to the vapour phase), activated intermediates for further decomposition and the re-organization of the solid matrix. Therefore, the process is a complex mechanism because consecutive and parallel paths act in a very narrow range of temperatures. The global behaviour can be studied in thermal analysis developing procedures commonly accepted for a useful characterization of the fuel. The thermogravimetric (TG) technique is the basis for a fundamental investigation and gives the fingerprinting of the fuel. It provides important characteristics (temperature of devolatilization, volatile matter released), reaction kinetics and significant parameters for preliminary modelling.

The subsequent phase of the fuel characterization should evaluate the effect of the operating conditions to give a more detailed and complete information on the devolatilization. In fact, the thermal history of solid fuels influences strongly the devolatilization parameters [6–9]. Although different specific experimental techniques should be compared to widening the range of conditions to those of large scale applications, a coherent fundamental study is required in the first phase of the characterization. Recent experimental thermogravimetric analyzers can reach very high temperatures and guarantee a negligible discrepancy between the programmed thermal history and the effective sample temperature in a relatively wide range of heating rate (HR). Nevertheless, a preliminary study should be carried out to minimize the heat transfer problems:

- limitation of temperature gradients in the sample testing a low amount of sufficiently fine particles,
- feed of relatively high gas flow rate to avoid secondary reactions,
- evaluation of buoyancy effects.

Therefore, the first aim of this work is to perform a fundamental study on the devolatilization of biomass residues, determine the most suitable and representative parameters and evaluate the effect of the operating conditions.

---

* Corresponding author. Tel.: +39 0502217850; fax: +39 0502217866.
E-mail address: e.biagini@ing.unipi.it (E. Biagini).

0040-6031/$ – see front matter © 2008 Elsevier B.V. All rights reserved.
doi:10.1016/j.tca.2008.03.015

From literature works, in low heating rate analyses (1–10 K/min), temperatures as low as 480 K are sufficient to begin the devolatilization of some biomasses, especially those containing extractive species. Natural polymers actually require somewhat higher temperatures for decomposition. Cellulose is the most studied component, with a good agreement on the devolatilization parameters (the starting temperature is in the range 570–600 K, the temperature for the maximum reaction rate is 630–660 K [10]) and the activation energy (195–213 kJ/mol [11,12] even though values in the range 50–250 can be found [10]). Hemicellulose is more reactive than cellulose, while lignin decomposes in a very large range of temperature (it may start at 540 K and end at 700 K [13]). Even in the relatively simple devolatilization of chemical compounds, the weight loss continues for temperature up to 1200 K [6,13,26]. This can be observed in the long tail of the TG curve at high temperature and the non-zero value of the derivative weight loss (dtg) after the main peak of devolatilization. This behaviour is not generally ascribed to any further component. The continuous release of volatile matter in the "secondary devolatilization" can be imputed to the decomposition at higher temperature of the rearranged structure of the solid after the primary devolatilization, occurred at lower temperature.

When biomass devolatilization is studied in a thermogravimetric balance, the different behaviour of the chemical components is revealed from a composite profile in the devolatilization curve. The contribution of each component can be recognized and this evidence is the basis of summative models, based on the hypothesis that the devolatilization proceeds independently from each others [14,15]. Each component is assumed to decompose according to a single first order reaction. Many modifications to this approach improve the model: the development of complex kinetic schemes instead of single first order reactions [6,11,16,17], the inclusion of further components [12], the imputation of the kinetic parameters to pseudo-components instead of chemical ones [18].

In all cases, the number of parameters in this approach is very high. This drawback could be surmounted if component parameters were valid for all biomass fuels. As a matter of fact, different celluloses, hemicelluloses, lignins can be recognized when different biomasses are analyzed. This depends on the chemical structure of natural polymers, their nature (the cristallinity of cellulose, for instance), their interconnection (that is how they are joined in the biomass matrix). Furthermore, the ash content in the biomass is ascertained to be crucial because it catalyzes and promotes the involved reactions [11,13,19]. As a matter of fact, the role of ashes is hardly modelled in summative models, while it should be quantified especially for biomass residues, having a high ash content.

Although commonly applied, the summative approach is actually an advanced level of modelling, requiring detailed investigation. Taking a step back, a simpler kinetic model should be directly developed from a fundamental study. Isoconversional methods are well established for obtaining kinetics from TG analysis [20]. Are they suitable for biomass devolatilization? Can they be useful for developing a fundamental kinetic model? Although originally developed for single reactions, later improvements enlarged the application to multi-step mechanisms and variable thermal history [21]. They need the results from different TG runs and allow the kinetics to be calculated without any assumption on the devolatilization model. For multi-step mechanisms the activation energy is not constant, being a complex sum of steps with different reactivity. Usually, the activation energy is reported as function of the conversion [19,22]. The average value may be considered as a measure of the devolatilization reactivity and inserted in a global reaction model. However, this level of approximation is not acceptable for biomass devolatilization. The starting temperature of devolatilization is generally overestimated with respect to the experimental determination. The long tail in the TG curve is roughly cut, with important errors on the final amount of volatile matter released. Only the intermediate steps of the main devolatilization process can be reasonably predicted.

Therefore, the second aim of this work is to perform a kinetic study on the devolatilization of biomass residues, test different isoconversional methods and develop a model implementing the kinetics as function of the conversion. Three biomass residues from food industry are studied by using a thermogravimetric balance. The effect of the heating rate (5–100 K/min) on devolatilization characteristics is evaluated. The kinetic study is carried out to compare the results from three traditional methods and comment on their applicability to biomass devolatilization. It is also the basis for elaborating the parameter input in the VEB model (Variable Energy activation model for Biomass devolatilization). A good agreement is obtained for all materials in the range of conditions studied.

2. Experimental

2.1. Materials

Three biomass fuels are studied, rice husks, olive cake (exhausted) and cacao shells. They were crushed and sieved and the fraction 90–125 μm used for the experimental runs. The proximate and ultimate analyses and the heating values of all materials are listed in Table 1.

2.2. Equipment

A thermogravimetric balance (TG Q500 V6.1 of TA Instruments) is used for all tests. The temperature range is from ambient to 1270 K, with heating rate from 0.1 to 100 K/min. The isothermal temperature precision is ±0.1 K. The thermocouple is positioned immediately adjacent to the sample. A second thermocouple is located slightly above the principal one. The weighing capacity is 1.0 g with a sensitivity of 0.1 μg. The purge gas is metered by mass flow controllers and set to 100 ml/min (STP). Pure nitrogen is used for the devolatilization tests.

2.3. Experimental method

The sample is loaded and dried at 380 K directly in the TG balance before each run. Usually, 5–10 min are sufficient to assure a constant weight of the sample. Then, a constant heating rate is programmed to 1220 K. At that temperature, the gas flow is switched to air and the carbonaceous residue is burnt. In all cases, two runs in the same conditions are carried out to confirm the good repro-

Table 1
Proximate and ultimate analyses and heating values of the materials

Fuel	Proximate analysis (% as received)				Ultimate analysis (% dry ash free)				HHV (MJ/kg)
	Moisture	VM	FC	ash	C	H	N	S	
Rice husks	10.74	59.83	15.85	13.57	51.18	7.34	0.85	0.18	15.53
Olive cake	5.64	70.74	21.41	4.95	55.13	7.43	1.87	0.23	18.47
Cacao shells	10.56	64.24	18.26	6.86	50.96	6.50	2.86	0.25	17.90

ducibility of the results. Negligible discrepancies are observed in the results reported here.

Seven heating rate programs are studied, 5, 10, 15, 20, 40, 60 and 100 K/min. Preliminary runs have been carried out to find the optimal conditions. In particular, the initial amount of sample is a crucial parameter to avoid significant heat transfer limitations in the entire range of HR. 5–6 mg was found to be the optimal initial sample mass.

2.4. Kinetic methods

The kinetic analysis of solid state decompositions is usually based on a single-step kinetic equation:

$$\frac{d\alpha}{dt} = A \exp\left(-\frac{E}{RT}\right) .f(\alpha) \tag{1}$$

where α is the extent of conversion, A and E the Arrhenius parameters, pre-exponential factor and activation energy, respectively, $f(\alpha)$ the reaction model, that is a function of α. Generally, the triplet A, E and $f(\alpha)$ are needed to define the kinetics of a reaction. Fit methods are used adopting a model and obtaining the Arrhenius parameters, which depend on the assumptions made. This approach may be useful only for the specific conditions used, devolatilization in other conditions (even on the same order of magnitude) being hardly predictable (see for instance Reynolds [19]). Therefore, fit methods are not tested here.

Model-free methods allow for evaluating the Arrhenius parameters without choosing the reaction model. In particular, the isoconversional methods yield the effective activation energy as a function of the extent of conversion. In the case of non-isothermal runs, they require a set of experimental tests at constant heating rate. This issue eliminates the compensation effects in determining the kinetic parameters. The knowledge of the dependence of E on α assists in both detecting multi-step processes and drawing certain mechanistic conclusions. Secondly, it is sufficient to predict the reaction kinetics over a wide temperature region. Three methods (Friedman [23], Flynn and Wall [24], Kissinger [25]) have been selected, because traditionally they have been applied to the decomposition of solids. The main equations are described in the following subsections.

According to Friedman [23], E/R can be obtained for a given value of α by plotting $\ln(d\alpha/dt)$ against $1/T$. This is a model-free method that can be applied to data sets obtained at different heating rates β:

$$\ln\left(\beta\frac{d\alpha}{dT}\right) = \ln A + \ln f(\alpha) - \frac{E}{RT} \tag{2}$$

This is a differential method, which can be applied to integral data (e.g. TG data) only after their numerical differentiation. In his original analysis, Friedman considered only the possibility that there was a single nth-order reaction present. If the value of E varies with the extent of conversion, the results should be interpreted in terms of multi-step reaction mechanisms.

According to the method of Flynn [24], E/R can be obtained by plotting $\ln(\beta)$ against $1/T$. This is a model-free method that can be applied measuring the temperatures corresponding to fixed values of α from experiments at different heating rates β:

$$\ln(\beta) = \ln\left[A\frac{f(\alpha)}{d\alpha/dT}\right] - \frac{E}{RT} \tag{3}$$

If E varies with α, the results should be interpreted in terms of multi-step reaction mechanisms.

The activation energy can be determined by the Kissinger method [25] without a precise knowledge of the reaction mechanism, using the following equation:

$$\ln\frac{\beta}{T_m^2} = \ln\left[A\cdot\frac{R}{E}\right] - \frac{E}{RT_m} \tag{4}$$

where T_m is the temperature at the maximum weight loss rate. This is actually a special case of obtaining E and A by considering T_m at different heating rate.

3. Results and discussion

3.1. Devolatilization parameters

The derivative weight loss curves of all materials are compared in Fig. 1 for 3 heating rates, 5, 20 and 100 K/min. Important infor-

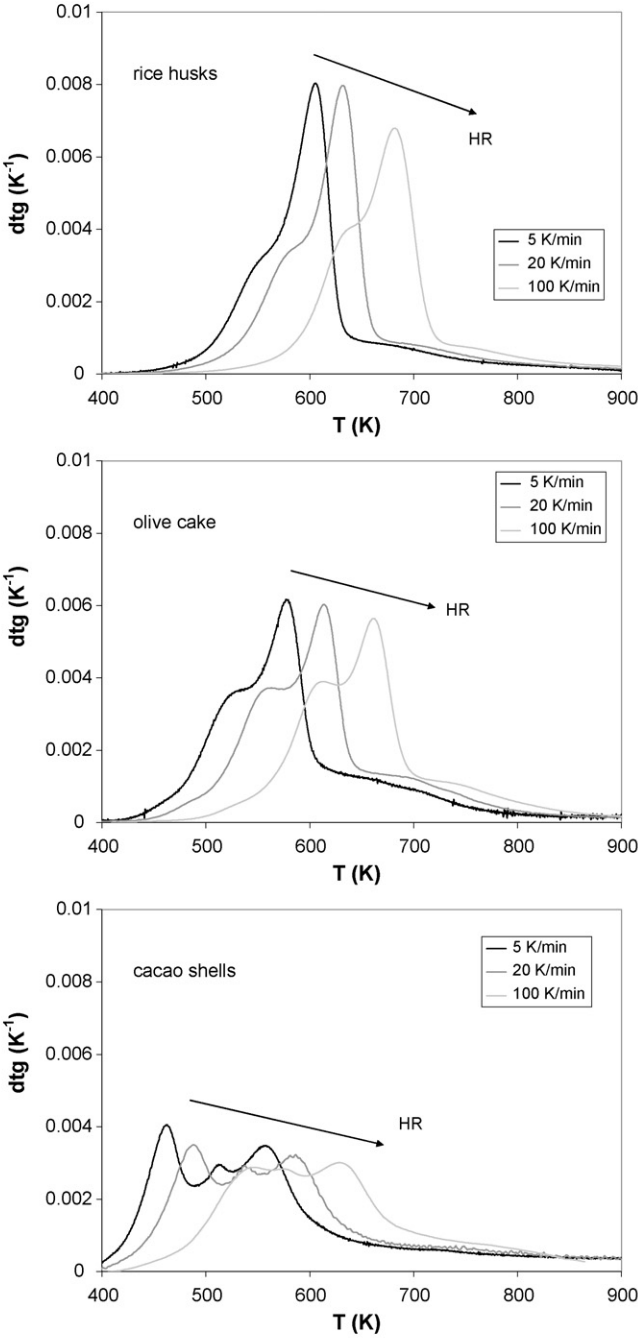

Fig. 1. Comparison of dtg curves for the biomass residues.

mation can be drawn from the analysis of these curves. First of all some parameters are defined or adopted from literature to quantify the effect of the heating rate on the devolatilization. The temperature T_m is defined as the temperature at the maximum weight loss rate dtg_m: these parameters are useful for comparing different materials, measure the fuel reactivity [19] and are the basis for some kinetic analysis (e.g. Kissinger method). The value of the conversion α_m at this temperature is also provided. As a matter of fact, different relative maxima may be observed in the dtg curves, the absolute maximum depending on the operating conditions (see the case of cacao shells). In these cases, a deeper investigation is required for a better comprehension of devolatilization phenomena. In general, the analysis of sub-peaks is performed (using deconvolution procedures) and each peak ascribed to the decomposition of chemical components or pseudo-components (extractives, cellulose, hemicellulose and lignin in the case of biomass fuels).

The onset temperature T_{onset} of devolatilization was originally defined as the intersection of the tangents to TG curve [10]. This parameter quantifies the temperature at which the devolatilization can be considered to start. For composite materials, the origin point to draw the tangent may be non-univocal, especially for multi-peak dtg curves. So, the definition of Gronli et al. [12] is adopted here: the onset temperature is the earliest relative maximum in the second derivative of the weight loss curve during the devolatilization of the dry material. The "tangent definition" may be more efficacious from a graphical point of view but to the detriment of reproducibility. For the materials considered here, T_{onset} obtained according to the "tangent definition" is 10–20 K lower than that obtained with the second definition.

Analogously, the offset temperature T_{offset} of devolatilization is defined as the latest relative minimum in the second derivative of the weight loss curve. This definition gives value 10–40 K lower than those obtained with the "tangent definition". This choice is motivated by the difficulty in defining the tangent line in the tail zone. The parameter T_{offset} quantifies the temperature at which the main devolatilization can be considered complete. For higher temperatures, a secondary devolatilization acts, responsible of a smaller weight loss (though not negligible) with respect to the main devolatilization [13,26]. The value of the conversion at this temperature α_{offset} is also provided to quantify the amount of volatile matter released in the main devolatilization, while the complementary value $(1-\alpha_{\mathrm{offset}})$ defines the amount of volatiles which will be released in the tail zone.

Weight loss, derivative and second derivative curves of cacao shells at 60 K/min are reported in Fig. 2 for simplifying the parameter definition. Two relative maxima T_{m1} and T_{m2} can be actually detected during the main devolatilization of this material. The difference between the values of the onset temperature using the two definitions above is also remarked.

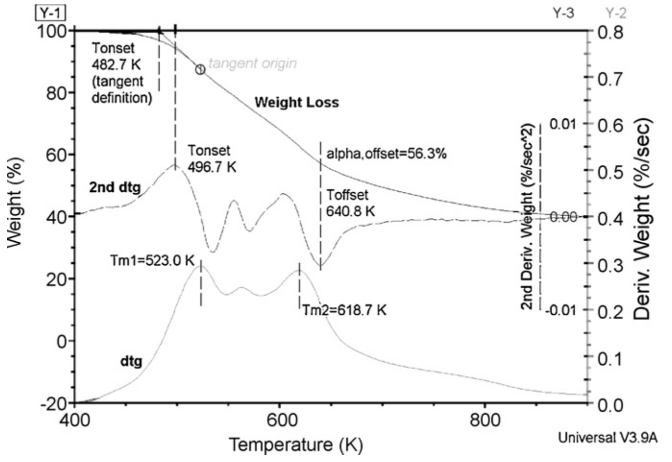

Fig. 2. Definition of devolatilization parameters (solid black curve: weight loss; solid grey curve: derivative; dashed black curve: second derivative).

The devolatilization parameters obtained for the biomass residues in the runs at 5, 20, 60 and 100 K/min are listed in Table 2 and discussed below.

The devolatilization profile of rice husks in Fig. 1 exhibits a complex peak with a well-defined main peak, a shoulder at earlier temperatures and a long tail zone. The higher the heating rate, the higher the values of T_{onset}, T_m and T_{offset}. For instance, the onset temperature is 530 K at 5 K/min, while it is 617 K at 100 K/min. The trend is quite linear on a logarithmic scale (Fig. 3). This can be useful for correlating the devolatilization parameters to the operating conditions. Observing the dtg curves in Fig. 1, dtg_m slightly decreases with HR. Vice versa, the shoulder at earlier temperatures becomes more and more important. Furthermore, at 5 K/min it is less evident than at 100 K/min. This means that the reactivity of the first two components (hemicellulose and cellulose) is differently influenced by the heating rate. At low HR, the dtg sub-peak of hemicellulose (at lower temperature than T_m, thus representing a shoulder of the main devolatilization peak) is almost incorporated in the main peak of cellulose, while at high HR the relative distance is larger and the separation of peaks more evident. The tail zone is confirmed by the value of the dtg, which is different from zero for temperatures higher than T_{offset}, while α_{offset} is between 66 and 70% (meaning that more than 30% of the volatile matter will be released in the tail zone).

Table 2
Effect of the heating rate on the devolatilization parameters

Fuel	HR (K/min)	T_{onset} (K)	T_m (K)	T_{offset} (K)	α_m (%)	α_{offset} (%)	dtg_m dry (%/K)
Rice husks	5	529.8	605.5	619.0	53.8	66.3	0.798
	20	559.5	631.9	646.9	55.0	68.1	0.790
	60	593.6	662.7	680.8	55.1	69.3	0.720
	100	616.6	681.8	700.1	56.5	70.0	0.678
Olive cake	5	499.2	577.1	591.2	46.9	56.9	0.616
	20	536.7	613.6	627.5	50.8	61.2	0.603
	60	568.2	644.6	662.6	51.6	61.7	0.572
	100	590.0	661.7	675.9	52.3	62.6	0.564
Cacao shells	5	448.3	462.7 (555.6)*	579.4	13.2 (45.0)*	53.3	0.404 (0.347)*
	20	469.5	488.3 (586.3)	607.7	13.8 (46.4)	53.5	0.351 (0.321)
	60	496.7	523.0 (618.7)	640.8	16.1 (48.2)	55.5	0.323 (0.313)
	100	506.4	545.5 (628.9)	659.0	17.4 (46.8)	56.3	0.287 (0.300)

* Values in brackets are obtained for the second sub-peak in the dtg profile of cacao shells (see Fig. 2).

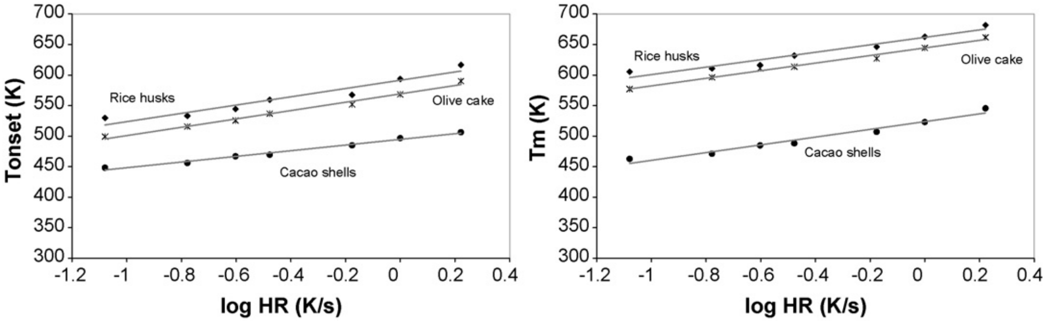

Fig. 3. Onset temperature and temperature at the maximum devolatilization rate of the biomass residues as functions of the heating rate.

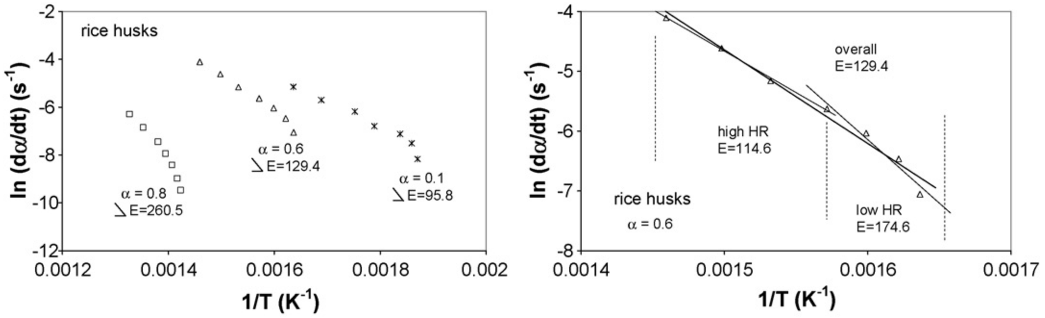

Fig. 4. Example of calculating the activation energy (reported in kJ/mol) at different conversion by the Friedman method.

Similar results can be drawn comparing the dtg curves of olive cake at various HR. However, generally, characteristic temperatures are lower with respect to rice husks. For instance, the onset temperature is 25–30 K lower for the devolatilization at the same heating rate. Approximately, 20 K is the difference of T_m for these materials. Although the peak of the main devolatilization is well defined, the shoulder at earlier temperatures is more evident for olive cake than rice husks, and again it becomes more evident at high HR. The tail zone is more remarked for this material, the conversion α_{offset} being approximately 60% at T_{offset}, which is approximately 20 K lower than that of rice husks.

The devolatilization behaviour of cacao shells differ qualitatively from the other two materials, a dtg peak of the main devolatilization being not evident. At least three sub-peaks of comparable intensity can be observed in Fig. 1. Furthermore, the temperature range of devolatilization (which can be defined as the difference between offset and onset temperatures) is wider than the other two materials. In particular, the onset temperature is very low, 448 K at 5 K/min. Two values of T_m are listed in Table 2, because at low HR the first peak is the absolute maximum, while at high HR the second peak is the absolute maximum. The offset temperature is not well defined, variations in the weight loss curve being hardly detectable. Considering the relative minimum in the second derivative, a conversion of 53–56% is achieved at T_{offset}, secondary devolatilization is hence very important.

3.2. Devolatilization kinetics

The temperature-conversion data are elaborated according to the specific method needs for the kinetic analysis. An example of the graphs obtained for a material is reported in Fig. 4. Similar graphs are obtained for all materials. For both Friedmann and Flynn methods, E varies strongly with the extent of conversion. An average value can be calculated (in the range 0.05–0.8) for both methods and compared with the activation energy obtained by using the Kissinger method. The results are listed in bold in Table 3. Results from Friedman and Flynn methods are comparable and similar values of the activation energy can be found in literature for the same materials. Values obtained by using the Kissinger method are quite different, usually lower than those from the other methods. In the case of cacao shells, the activation energy is even 2 times lower for Kissinger method with respect to the others. This result can be explained considering how the Kissinger method works. It focuses on the temperature at the maximum weight loss rate. The ideal case should be a single reaction, which could be studied following this parameter. However, as described in the previous section, the biomass devolatilization is a very complex sum of reactions, which can be hardly studied by following the temperature for the maximum decomposition rate. As depicted also in Fig. 1, the dtg profile of cacao shells is very different from a single reaction, several sub-peaks being detectable. Even, the peak with T_m (the temperature at the absolute maximum devolatilization rate) at 5 K/min is

Table 3
Comparison of the activation energy obtained by using different isoconversional methods (low HR = 5–20 K/min, high HR = 20–100 K/min, overall = 5–100 K/min)

Fuel	Friedman			Flynn			Kissinger		
	Low HR	High HR	Overall	Low HR	High HR	Overall	Low HR	High HR	Overall
Rice husks	182.2	118.8	135.5	169.0	110.7	128.1	140.8	101.3	112.5
Olive cake	150.0	106.5	119.1	141.6	103.2	117.8	94.4	76.4	103.2
Cacao shells	133.7	119.3	127.7	145.6	117.8	129.6	83.3 (106.4)*	53.1 (102.5)*	65.3 (104.8)*

* Values in brackets are obtained for the second sub-peak in the dtg profile of cacao shells.

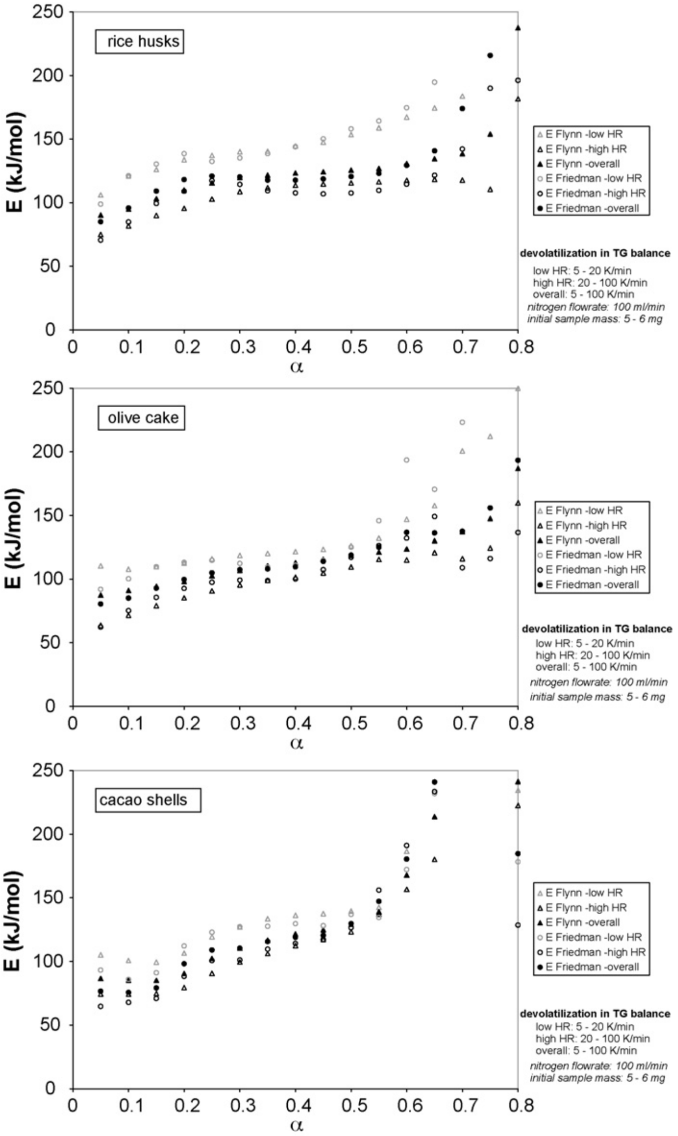

Fig. 5. Comparison of the activation energy obtained by using different kinetic methods for the devolatilization of the biomass residues.

different from the peak with T_m at 100 K/min. Nevertheless, also considering correspondent peaks and the respective temperatures, the results (reported in Table 3) are questionable. Also for rice husks and olive cake, the results are hardly reliable, even though the dtg profiles are more similar to a single reaction profile. Finally, the Kissinger method is hardly suitable for calculating the kinetics of devolatilization of biomass residues.

Although average values of the activation energy may be sufficient for a preliminary approximation of biomass devolatilization, the function $E(\alpha)$ gives a more accurate description and allows devolatilization steps to be studied. Solid symbols in Fig. 5 represent the activation energy for all materials. Friedman and Flynn methods give comparable results. Discrepancies can be observed for conversions higher than 0.7 and in the very initial steps of devolatilization (conversion around 0.05–0.1). For intermediate values of the conversion, the results of both methods agree well enough. The trend of these curves depends on the material. In general, E increases in the first steps for α up to 0.2. A *plateau* can be observed for values of α between 0.25 and 0.55 in the case of rice husks, while in the case of the other materials a moderate increase of E with the conversion can be observed in this range, instead of a real *plateau*. For higher values of α, the activation energy increases strongly up to values even twice those observed in the *plateau*.

In any case, the activation energy increases significantly in the entire range of conversion. Smaller values of the average E mean a more reactive solid, while larger values mean a less reactive solid. This may explain the devolatilization behaviour of most biomass fuels, which contain reactive components responsible of the initial steps of devolatilization, while the final tail of devolatilization can be caused by the less reactive structure of the remaining solid after the main devolatilization.

The activation energy is a property of a specific reaction and should not depend on the operating conditions. However, the global value of the activation energy obtained in the case of biomass fuel devolatilization is a complex sum of several reactions. The heating rate of the sample may favour a reaction with respect to competitive ones. For instance, as reported by Maciejewski [27] reactions A and B, described with respective kinetics, may have identical temperature-conversion curves at 5 K/min, while at lower HR reaction A is faster, vice versa at higher HR reaction B is favoured. This may explain the increased distance in the hemicellulose and cellulose sub-peaks observed in the dtg profiles in Figs. 1 at 5 and 100 K/min, for rice husks and olive cake.

In biomass devolatilization, only a global activation energy can be studied, which is a complex sum of more or less favoured reactions, depending on the heating rate. Isoconversional methods take into account the heating rate for non-isothermal tests, isolating the parameter β in Eq. (2–4). Nevertheless, a sensible dependence of E with the heating rate can be observed. In the previous kinetic analysis, we used 7 tests for each material to obtain the activation energy. More than a few tests are recommended in isoconversional analysis to reduce errors due to experimental uncertainty and heat transfer limitations during the test. Usually, 4 tests are sufficient in kinetic analysis. Therefore, the results obtained so far have been divided in two sets of data, low (5–20 K/min) and high (20–100 K/min) heating rate, respectively. The activation energy obtained for both sets can be compared with values obtained for the overall range of HR. An example of calculation and a graphical comparison can be observed in Fig. 4 in the specific case of rice husks, Friedman method and fixed conversion 0.6. Least squares lines giving the value of E differ significantly. The average values (for conversion in the range 0.05–0.8) of the activation energy obtained at low HR, high HR and overall are listed in Table 3 for all materials and methods. The value of E is higher at low HR and lower at high HR with respect to overall values, for all materials and using all methods.

Similar conclusions have been drawn in literature works for the decomposition of biomass materials. Even in the case of cellulose, the most simple biomass component, Milosavljevic and Suuberg [28], reviewing the global kinetics of cellulose pyrolysis, recognized two sets of values: around 218 kJ/mol at low HR (<10 K/min), 140 kJ/mol at high HR (>10 K/min) and isothermal runs. The authors suggested the existence of two regimes, depending on the conditions used. Gronli et al. [29] found a similar conclusion when comparing the activation energy obtained during the decomposition of cellulose at 5 K/min (244 kJ/mol) and at 40 K/min (222 kJ/mol). However, they commented that the thermal lag was largely responsible for the decrease in values of E and log A at higher heating rates.

The effect of HR is not only observable in the average values of E. More detailed results can be observed in Fig. 5, where $E(\alpha)$ curves at low HR, high HR and overall are compared for both methods and all materials. The largest deviations between values at low and high HR are generally observed in the earlier steps (conversion 0.05–0.2) and at high conversions. These deviations can be due to the sensitivity of differential methods (which employ instantaneous rate

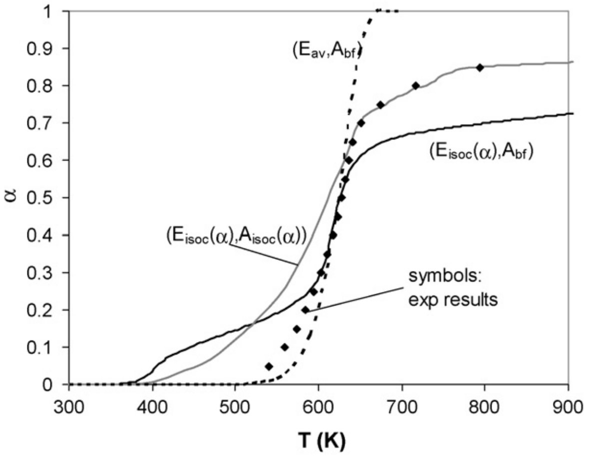

Fig. 6. Comparison of curves obtained by using different approaches in modelling the devolatilization as a single first order reaction and the experimental results obtained for rice husks at 20 K/min. (E_{av}, A_{bf}) are the kinetics not dependent on the conversion, average activation energy from the Friedman method and pre-exponential factor from the best-fit, respectively. ($E_{isoc}(\alpha)$, A_{bf}) are the kinetics with the activation energy function of the conversion from the Friedman method and pre-exponential factor from the best-fit, respectively. ($E_{isoc}(\alpha)$, $A_{isoc}(\alpha)$) are the kinetics dependent on the conversion, both from the Friedman method.

values) to experimental noise [30]. Furthermore, the characteristic equations of the isoconversional methods are derived assuming a constant activation energy. This assumption introduces some systematic error in estimating $E(\alpha)$, especially when this latter varies significantly.

3.3. Development of the VEB (Variable activation Energy model for Biomass devolatilization) model

Although the kinetic values depend on the conversion, the operating conditions and the method used, can the isoconversional methods represent the basis for a fundamental kinetic model, useful for direct applications? As discussed above, a single first order reaction model (assuming an average value E_{av} of the activation energy) can give only a representation of the main devolatilization, but hardly can give a description of the earlier devolatilization and the long final tail. However, it is the simplest model, easy to be included in comprehensive codes for combustion and gasification, and therefore, some modifications may improve the approach to benefit these features.

As a first step, the average values of the activation energy obtained by using the three methods are input in a first order reaction model (assuming $f(\alpha) = 1 - \alpha$ in Eq. (1)). The pre-exponential factor is calculated from the best-fit with the experimental results of all set of runs (5–100 K/min). The experimental results are compared in Fig. 6 with the results of this preliminary attempt in the case of rice husks at 20 K/min. A scarce agreement is obtained: a difference of 25–30 K can be observed at the earlier conversions, but the most important divergence is for conversions higher than 0.7 and the final conversion. Similar qualitative considerations can be drawn for the other cases.

In the subsequent step, let define $E_{isoc}(\alpha)$ the activation energy directly obtained by using the isoconversional method (from the Friedman method in the following discussion, though the results from the Flynn method are qualitatively similar). A model with E variable with the conversion can be developed simply inserting $E_{isoc}(\alpha)$ in Eq. (1):

$$\frac{d\alpha}{dt} = A \exp\left(-\frac{E_{isoc}(\alpha)}{RT}\right).(1-\alpha) \qquad (5)$$

Although the isoconversional methods can give also the pre-exponential factor $A_{isoc}(\alpha)$, the first attempt is made by considering a fixed value of A obtained from the best-fit of the experimental results by using $E_{isoc}(\alpha)$ in the entire range. This approach gives results (see Fig. 6) even worse than those of the previous approach with the average value E_{av}. In fact, in the earlier steps the value of $E_{isoc}(\alpha)$ is very low giving unrealistic low onset temperatures. Vice versa, in the tail zone, the value of $E_{isoc}(\alpha)$ is very high, causing the devolatilization to stop and underestimating the final conversion. As a matter of fact, only at the intermediate values of the conversion the agreement is good.

A kinetic model with both parameters variable with the conversion, although quite complex, gives not more appreciable results. $A_{isoc}(\alpha)$ (here calculated according to the Friedman method) is a curve qualitatively similar to that of the correspondent $E_{isoc}(\alpha)$. The comparison of the results of this approach with the previous cases and the experimental results is also reported in Fig. 6. In this case, only the very final part of the curve agrees with the experimental results. Disagreements are observed also for the other materials and HR runs.

So, as a first conclusion, the kinetic parameters obtained by using the isoconversional methods are not directly applicable and a further step should be elaborated. The function $E_{isoc}(\alpha)$ in Eq. (5) can be modified to give a more satisfying fit of the experimental results. Bearing in mind the comments above on the systematic errors of the isoconversional methods, the intermediate values of $E_{isoc}(\alpha)$ can be preserved, selecting an interval [α1,α2] of the main devolatilization where the experimental noise is low and the activation energy is a weak function of the conversion (see the *plateau* in Fig. 5). After a preliminary investigation, the best results are obtained by using $E_{isoc}(\alpha)$ in the interval [α1,α2] to calculate the value of A from the best-fit of the experimental results, limiting the comparison to this interval of α (see the scheme in Fig. 7). The best-fit is calculated minimizing the sum of errors between calculated and experimental results, extending the sum to all HR runs (5–100 K/min). Subsequently, two values of E are fixed for $\alpha = 0.05$ (E_{on}) and $\alpha = 0.8$ (E_{off}). An appropriate function then should be defined to link the points (0.05, E_{on}) and (0.8, E_{off}) and the points of $E_{isoc}(\alpha)$ in [α1,α2]. A suitable function is a cubic which best interpolates these points. Let define this function $E_{cub}(\alpha)$ in the range [0,1]. Finally, $E_{VEB}(\alpha)$ is defined in three intervals as shown in the scheme of Fig. 7.

$E_{isoc}(\alpha)$ is then substituted with $E_{VEB}(\alpha)$ in Eq. (5), which is numerically integrated and the results compared with the experimental curves. The procedure is optimized by considering the widest interval [α1,α2] for each material and varying E_{on} and E_{off} till the characteristic temperatures (T_{onset} and T_{offset}, respectively) obtained during the previous characterization are matched for all HR runs.

The resulting function $E_{VEB}(\alpha)$ and the correspondent values of A are reported in Fig. 8 for all materials. The optimal interval [α1,α2] is [0.2,0.55] for rice husks, [0.2,0.45] for olive cake, [0.25,0.5] for cacao shells, respectively. The deviations with respect to $E_{isoc}(\alpha)$ reported in Fig. 5 are remarkable at the earlier conversions and in the tail zone, $E_{VEB}(\alpha)$ exhibiting milder variations. For all materials, E_{on} results between $E_{isoc}(0.05)$ and $E_{isoc}(\alpha 1)$, while E_{off} results between $E_{isoc}(\alpha 2)$ and $E_{isoc}(0.8)$.

Finally, the comparison of the experimental results and the results of the VEB model is reported in Fig. 9 for all materials. The agreement is good for all runs. Also reported is the deviation defined according to the following equation:

$$\text{dev}(\%) = \frac{\sum_N \left|\alpha_{VEB} - \alpha_{exp}\right|}{N} \times 100 \qquad (6)$$

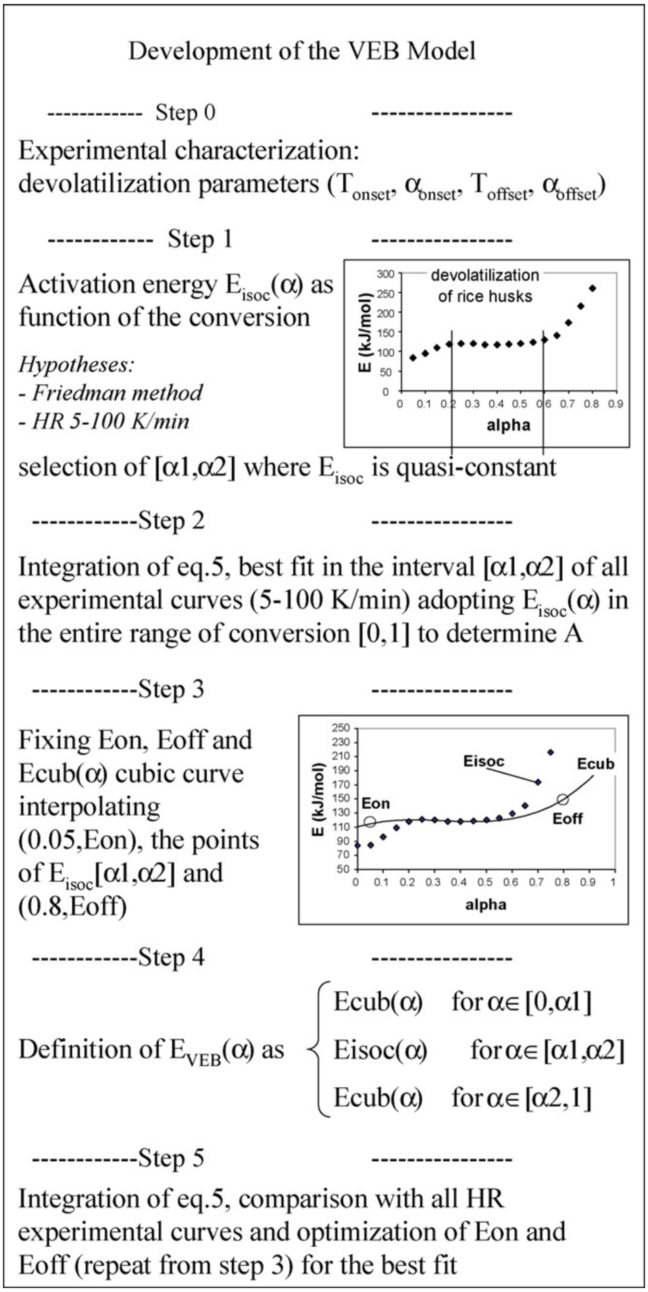

Development of the VEB Model

------------ Step 0 ----------------

Experimental characterization: devolatilization parameters (T_{onset}, α_{onset}, T_{offset}, α_{offset})

------------ Step 1 ----------------

Activation energy $E_{isoc}(\alpha)$ as function of the conversion

Hypotheses:
- Friedman method
- HR 5-100 K/min

selection of [α1,α2] where E_{isoc} is quasi-constant

------------Step 2 ----------------

Integration of eq.5, best fit in the interval [α1,α2] of all experimental curves (5-100 K/min) adopting $E_{isoc}(\alpha)$ in the entire range of conversion [0,1] to determine A

------------Step 3 ----------------

Fixing Eon, Eoff and Ecub(α) cubic curve interpolating (0.05,Eon), the points of E_{isoc}[α1,α2] and (0.8,Eoff)

------------Step 4 ----------------

$$\text{Definition of } E_{VEB}(\alpha) \text{ as } \begin{cases} \text{Ecub}(\alpha) & \text{for } \alpha \in [0,\alpha 1] \\ \text{Eisoc}(\alpha) & \text{for } \alpha \in [\alpha 1,\alpha 2] \\ \text{Ecub}(\alpha) & \text{for } \alpha \in [\alpha 2,1] \end{cases}$$

------------Step 5 ----------------

Integration of eq.5, comparison with all HR experimental curves and optimization of Eon and Eoff (repeat from step 3) for the best fit

Fig. 7. Scheme of the VEB model.

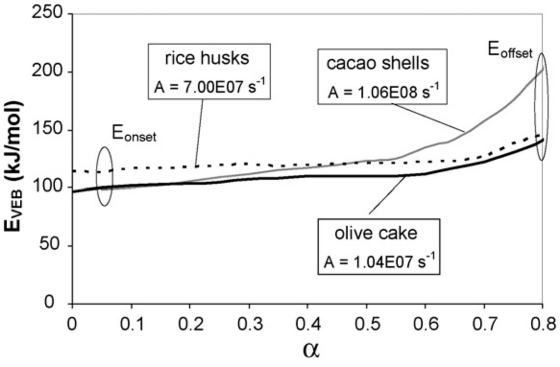

Fig. 8. E_{VEB} curves and optimized values of A for the biomass residues.

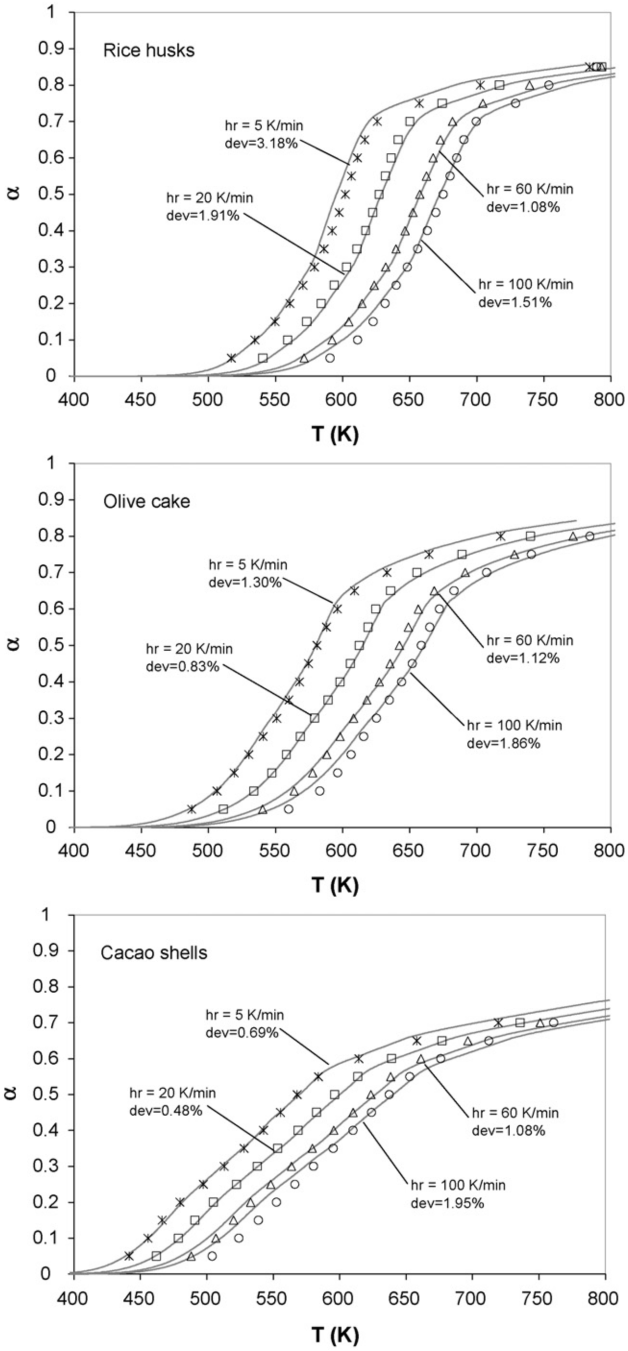

Fig. 9. Comparison of the experimental results and results of the VEB model for the biomass residues in four HR runs. dev is defined in Eq. (6).

where N is the number of results considered. The procedure described in Fig. 7 is repeated to minimize the sum of all dev(%) in the range 5–100 K/min.

It is worth noting that the specific behaviour of the material in the devolatilization curves is guaranteed by adopting $E_{isoc}(\alpha)$ in the main devolatilization interval [α1,α2], which is a result of the fundamental study reported in the previous section. This is not really constant, but varies weakly with the conversion allowing the composite shape of the main devolatilization to be well-predicted.

The results of the VEB model are good and derive mainly from a fundamental study. A simple kinetic scheme is adopted without assuming any chemical or pseudo-components, even though the multi-step mechanism can be studied. Moreover, although the trend of E_{VEB} for cacao shells is a little steeper than the other residues, many similarities can be observed in the curves of Fig. 8. So, a generalization of the approach could be pursued: it would require to enlarging the number of biomass studied and maybe grouping those of the same origin and nature.

4. Conclusions

The devolatilization is the basic step of thermochemical processes and requires a fundamental characterization. The devolatilization of three biomass residues (rice husks, olive cake, cacao shells) was studied in a TG balance. Significant parameters were defined for giving the fingerprinting of the fuel and comparing different cases. The effect of the heating rate was evaluated in the range 5–100 K/min. Graphical correlations were provided for the onset temperature and the temperature at the maximum devolatilization rate. Traditional isoconversional methods were applied to all residues and the kinetics obtained as functions of the conversion. The trend of $E(\alpha)$ curve is an index of the multi-step nature of the biomass devolatilization. In particular, the main devolatilization was characterized by a quite constant value of the activation energy, while it is lower at earlier conversion. Higher values of E (with respect to the average value) explained the long tail in the curve typical at high conversion. As previously reported in literature works, the activation energy was found to depend also on the HR, considering the average values as well as the entire curve $E(\alpha)$. Although average values allowed the reactivity of different fuels to be compared ($E = 135.5$ kJ/mol for rice husks, 119.1 for olive cake, 127.7 for cacao shells), a first order reaction model can hardly predict the biomass devolatilization. A VEB model has been developed, basing on the results of the isoconversional methods. The value of E at onset and offset conversions were optimized and linked to $E(\alpha)$ limited to the main devolatilization interval. A good agreement was obtained for the biomass residues in all HR runs in the entire range of temperatures. Similarities in the optimized E_{VEB} curves for the three fuels of this work suggested to pursue a generalization in the approach, enlarging the number and variety of fuels studied.

Acknowledgement

This work collects part of the results of the Italian project FISR: “Integrated Systems for Hydrogen Production and Use in Distributed Generation”.

References

[1] T. Abbas, P.G. Costen, F.C. Lockwood, Symposium (Int.) on Combustion 26 (1996) 3041–3058.
[2] H. Spliethoff, K.R.G. Hein, Fuel Process. Technol. 54 (1998) 189–205.
[3] M. Sami, K. Annamalai, M. Wooldridge, Prog. Energy Combust. Sci. 27 (2001) 171–214.
[4] A.V. Bridgwater, Chem. Eng. J. 91 (2003) 87–102.
[5] T.F. Wall, Proc. Combust. Inst. 31 (2007) 31–47.
[6] J.A. Caballero, J.A. Conesa, R. Font, A. Marcilla, J. Anal. Appl. Pyrolysis 42 (1997) 159–175.
[7] L.P. Wiktorsson, W. Wanzl, Fuel 79 (2000) 701–716.
[8] E. Biagini, C. Fantozzi, L. Tognotti, Combust. Sci. Technol. 176 (2004) 685–703.
[9] M. Otero, X. Gómez, A.I. García, A. Morán, Chemosphere 69 (2007) 1740–1750.
[10] S. Gaur, T.B. Reed, Thermal Data for Natural and Synthetic Fuels, Marcel Dekker Inc., New York, 1998.
[11] G. Varhegyi, M.J. Antal, E. Jakab, P. Szabó, J. Anal. Appl. Pyrolysis 42 (1997) 73–87.
[12] M.G. Gronli, G. Varhegyi, C. Di Blasi, Ind. Eng. Chem. Res. 41 (2002) 4201–4208.
[13] E. Biagini, F. Barontini, L. Tognotti, Ind. Eng. Chem. Res. 45 (2006) 4486–4493.
[14] C.A. Koufopanos, G. Maschio, A. Lucchesi, Can. J. Chem. Eng. 67 (1989) 75–84.
[15] K. Raveendran, A. Ganesh, K.C. Khilar, Fuel 75 (1996) 987–998.
[16] J.J. Manya, E. Velo, L. Puigjaner, Ind. Eng. Chem. Res. 42 (2003) 434–441.
[17] S. Hu, A. Jess, M. Xu, Fuel 86 (2007) 2778–2788.
[18] J.J.M. Orfao, F.J.A. Antunes, J.L. Figueiredo, Fuel 78 (1999) 349–358.
[19] J.G. Reynolds, A.K. Burnham, Energy Fuels 11 (1997) 88–97.
[20] M.E. Brown, M. Maciejewski, S. Vyazovkin, et al., Thermochim. Acta 355 (2000) 125–143.
[21] S. Vyazovkin, J. Comput. Chem. 18 (1997) 393–402.
[22] R. Capart, L. Khezami, A.K. Burnham, Thermochim. Acta 417 (2004) 79–89.
[23] H.L. Friedman, J Polym. Sci. 50 (1965) 183–195.
[24] J.H. Flynn, L.A. Wall, J. Res. Nat. Bur. Stand. 70A (1966) 487–493.
[25] H.E. Kissinger, Anal. Chem. 29 (1957) 1702–1706.
[26] T. Fisher, M. Hajaligol, B. Waymack, D. Kellogg, J. Anal. Appl. Pyrolysis 62 (2002) 331–349.
[27] M. Maciejewski, Thermochim. Acta 355 (2000) 145–154.
[28] I. Milosavljevic, E.M. Suuberg, Ind. Eng. Chem. Res. 34 (1995) 1081–1091.
[29] M. Gronli, M.J. Antal, G. Varhegyi, Ind. Eng. Chem. Res. 38 (1999) 2238–2244.
[30] S. Vyazovkin, J. Comput. Chem. 22 (2001) 178–183.